

## Effect of top quark spin on the $Wtb$ couplings in $e^+p$ collisions

S. Atağ\* and B. Şahin†

*Department of Physics, Faculty of Sciences, Ankara University, 06100 Tandogan, Ankara, Turkey*  
(Received 8 July 2005; published 3 April 2006)

In our previous work [Phys. Rev. D **70**, 037503 (2004)] for the  $e^+p \rightarrow t\bar{\nu} + X$  process, we have shown that the top quark possesses a high degree of spin polarization when its spin decomposition axis is along the incoming lepton beam. In this work, the potential of  $ep$  collisions to probe an anomalous  $Wtb$  vertex is investigated via the polarized single top quark production process for TESLA + HERAp energy. The effects of the top quark polarization to  $Wtb$  couplings  $F_{2L}$  and  $F_{2R}$  are discussed. It is possible to define a polarization axis for the top quark that is more sensitive to new physics than the unpolarized case.

DOI: [10.1103/PhysRevD.73.074001](https://doi.org/10.1103/PhysRevD.73.074001)

PACS numbers: 14.65.Ha, 13.88.+e

### I. INTRODUCTION

The physics of top quarks needs more investigation because of its prominent heavy mass and couplings to other particles such as vector bosons, Higgs scalars, and fermions. More accurate measurements of the top quark properties are valuable as an input to precision electroweak analyses. The top quark may be useful to discover new physics. For example, Higgs boson couples most strongly to the top quark rather than other known fermions. Since the coupling  $Wtb$  is responsible for all top quark decays, it plays a crucial role to help understand the nature of electroweak theory and “new physics” beyond. Therefore it is important to study the  $Wtb$  vertex and measure the coupling parameters with high precision. Single top quark production processes provide a unique possibility to search for this vertex due to their direct proportionality to the  $Wtb$  coupling. Deviations from the standard model (SM) expectation in the  $Wtb$  vertex would be a possible signal for the new physics beyond SM. In this work, the influence of the top quark polarization on the search for the anomalous  $Wtb$  couplings is investigated through the single top quark production in  $ep$  collision at TESLA + HERAp energy  $\sqrt{s} = 1.6$  TeV. Linear collider (LC) design TESLA at DESY would be an  $ep$  collider when LC is constructed on the same base as the proton ring. Estimations about the main parameters of this collider mode can be found in Ref. [1].

Several collider experiment potentials have been examined to search for these coupling parameters through single top production. Single top cross section for the process  $e^+e^- \rightarrow Wtb$  has been discussed below and above the  $t\bar{t}$  threshold [2,3] and for the process  $e^+e^- \rightarrow e\bar{\nu}tb$  at CERN  $e^+e^-$  collider LEP2 [4] and linear  $e^+e^-$  collider (LC) [5,6] energies. Investigations for the  $Wtb$  vertex have been done at  $\gamma e$  mode of LC [7], Fermilab  $p\bar{p}$  collider Tevatron, and CERN  $pp$  collider LHC [8,9]. Through the unpolarized top quarks in  $ep$  collision  $Wtb$  couplings were examined in Ref. [10].

In the model independent effective Lagrangian approach [11–14], there are seven anomalous  $CP$  conserving operators of dimension six which contribute  $Wtb$  vertex. This effective Lagrangian contains four independent couplings whose explicit forms are given in Ref. [13]. Effects of all seven operators will not be investigated here. We only consider the following couplings to reveal the potential of  $ep$  collision:

$$L = \frac{g_w}{\sqrt{2}} \left[ W_\mu \bar{t}(\gamma^\mu F_{1L} P_- + \gamma^\mu F_{1R} P_+) b - \frac{1}{2m_w} W_{\mu\nu} \bar{t} \sigma^{\mu\nu} (F_{2L} P_- + F_{2R} P_+) b \right] + \text{H.c.}, \quad (1)$$

where

$$W_{\mu\nu} = D_\mu W_\nu - D_\nu W_\mu, \quad D_\mu = \partial_\mu - ieA_\mu, \quad (2)$$

$$P_\mp = \frac{1}{2}(1 \mp \gamma_5), \quad \sigma^{\mu\nu} = \frac{i}{2}(\gamma^\mu \gamma^\nu - \gamma^\nu \gamma^\mu).$$

In the SM, the  $(V - A)$  coupling  $F_{1L}$  corresponds to the Cabibbo-Kobayashi-Maskawa matrix element  $V_{tb}$  which is very close to unity and  $F_{1R}$ ,  $F_{2L}$ , and  $F_{2R}$  are equal to zero. The  $(V + A)$  coupling  $F_{1R}$  is severely bounded by the CLEO  $b \rightarrow s\gamma$  data [15] at a level such that it will be out of reach at expected future colliders. Therefore we set  $F_{1L} = 0.999$  and  $F_{1R} = 0$  as required by present data [16]. The magnetic-type anomalous couplings are related to the coefficients  $C_{tW\Phi}$  and  $C_{bW\Phi}$  [13] in the general effective Lagrangian by

$$F_{2L} = \frac{C_{tW\Phi} \sqrt{2} v m_w}{\Lambda^2 g}, \quad F_{2R} = \frac{C_{bW\Phi} \sqrt{2} v m_w}{\Lambda^2 g}, \quad (3)$$

where  $\Lambda$  is the scale of new physics. Natural values of the couplings  $F_{2L(R)}$  are in the region [17] of

$$\frac{\sqrt{m_b m_t}}{v} \sim 0.1 \quad (4)$$

and do not exceed unitarity violation bounds for  $|F_{2L(R)}| \sim 0.6$  [12].

In  $ep$  collision the process for single top quark production is  $ep \rightarrow t\bar{b}\bar{\nu} + X$ . The subprocess contributing to the

\*Electronic address: atag@science.ankara.edu.tr

†Electronic address: dilec@science.ankara.edu.tr

process above is the  $W$  gluon fusion  $eg \rightarrow t\bar{b}\bar{\nu}$  ( $2 \rightarrow 3$  process), where a virtual  $W$  strikes a gluon to produce the  $t\bar{b}$  pair. If  $\bar{b}$  is nearly collinear with the incident gluon the  $b$  quark propagator blows up in the zero  $b$  mass limit. The  $b$  mass regulates the collinear divergence such that the resulting cross section is proportional to  $\alpha_s \ln(m_t^2/m_b^2)$ . In addition, each emission of a collinear gluon off the internal  $b$  quark produces another power of  $\alpha_s \ln(m_t^2/m_b^2)$ , because it yields another  $b$  propagator which is nearly on shell. Therefore, the expansion parameter for perturbation is  $\alpha_s \ln(m_t^2/m_b^2)$  rather than  $\alpha_s$ . This makes the perturbation theory less convergent and cross sections do not have a desired accuracy. A solution to this problem is to introduce the  $b$  quark distribution function in the proton where the collinear logarithms are resummed to all orders by the Dokshitzer-Gribov-Lipatov-Altarelli-Parisi equations at the scale  $\mu \sim m_t$ . So, the major part of the  $W$  gluon fusion process  $eg \rightarrow t\bar{b}\bar{\nu}$  with collinear enhancement can be reformulated by taking into account the process  $eb \rightarrow t\bar{\nu}$  ( $2 \rightarrow 2$  process) via  $t$ -channel  $W$  boson exchange. The rest of the cross section of  $eg \rightarrow t\bar{b}\bar{\nu}$  corresponding to the higher  $\bar{b}$  quark  $p_T$  values becomes a correction term to the process  $eb \rightarrow t\bar{\nu}$ . When the two processes  $2 \rightarrow 2$  and  $2 \rightarrow 3$  are combined together, one should avoid double counting due to the overlap region of the collinear case. In order to take care of this double counting, we use the method proposed in Ref. [18]. Then the combined cross section can be organized as follows:

$$\sigma = \sigma(eb \rightarrow t\bar{\nu}) + \sigma(eg \rightarrow t\bar{b}\bar{\nu}) - \sigma(g \rightarrow b\bar{b} * eb \rightarrow t\bar{\nu}), \quad (5)$$

where the subtracted term is the gluon splitting piece of the cross section for  $eg \rightarrow t\bar{b}\bar{\nu}$ .

Following the above discussion, we obtained in Ref. [19] dominant top quark spin polarization fractions from each of the processes  $eg \rightarrow t\bar{b}\bar{\nu}$ ,  $eb \rightarrow t\bar{\nu}$  and from a combination of them depending on the spin decomposition axes such as  $e$ -beam, proton-beam, and helicity direction. These results are shown in Table I at TESLA + HERAp energies. As can be seen from Table I single top quarks produced via  $eb \rightarrow t\bar{\nu}$  subprocesses possess complete spin polarization in terms of a basis which decomposes the top quark spin in its rest frame along the direction of the incoming  $e$ -beam. In this table LAB helicity refers to the  $ep$  center of mass system and ZMF stands for zero momentum frame which is the center of mass (cm) frame of the  $eb$  system. The spin fraction is defined as the ratio of the polarized cross section to the unpolarized one. It should be pointed out that the overlap region needs extra discussion. There are two possibilities to define ZMF which are in terms of either  $eg$  or  $eb$  initial states. Helicity of the top quark is not invariant under longitudinal boosts connecting these two frames. Therefore, it is not possible to define ZMF uniquely.

TABLE I. Dominant spin fractions and asymmetries for the various top quark spin bases in the production of the single top process with the  $Wg$  fusion channel at  $\sqrt{s} = 1.6$  TeV TESLA + HERAp energy. Contributions from each  $2 \rightarrow 2$  and  $2 \rightarrow 3$  process and combinations of them are listed.

Basis	$2 \rightarrow 2$	$2 \rightarrow 3$	Overlap	Total	$\frac{N_+ - N_-}{N_+ + N_-}$
LAB helicity	80%(R)	77%(R)	79%(R)	77%(R)	0.54
ZMF helicity	95%(L)	76%(L)	Undefined	Undefined	Undefined
$e$ -beam	100% $\uparrow$	93% $\uparrow$	98% $\uparrow$	96% $\uparrow$	0.92
Antineutrino	95% $\uparrow$	90% $\uparrow$	93% $\uparrow$	92% $\uparrow$	0.84
$p$ -beam	90% $\downarrow$	86% $\downarrow$	88% $\downarrow$	87% $\downarrow$	-0.75

Further difficulty arises from reconstructing ZMF experimentally due to the  $2 \rightarrow 3$  process with possible low- $p_T$  final state particles. Another point to mention is the opposite helicity directions between the ZMF and LAB frames observed in Table I. In  $ep$  collision, boosting from the ZMF to the LAB system brings a large difference in incoming  $b$  quark momenta because of the parton distribution in the proton. Then, the momentum of the positron is much more dominant in the LAB frame (since the LAB frame is defined as the cm frame of the  $ep$  system). This property can reverse the direction of the top momentum due to its heavy mass. Therefore, longitudinal boosting can reverse the top helicity.

## II. SPIN DEPENDENT CROSS SECTION AND TOP DECAY RATE

In this work we use only main subprocess  $e^+b \rightarrow t\bar{\nu}$  for the production of the single top quark for analytical simplicity and disregard correction from  $eg \rightarrow t\bar{b}\bar{\nu}$  which gives the minor contribution as seen in Table I. Let us start with the complete differential cross section including subsequent top decay

$$\begin{aligned} d\sigma(e^+b \rightarrow t\bar{\nu} \rightarrow \ell^+ b\bar{\nu}\nu_\ell) &= \frac{1}{2s} |M|^2 \frac{d^3 p_3}{(2\pi)^3 2E_3} \frac{d^3 p_4}{(2\pi)^3 2E_4} \\ &\times \frac{d^3 p_5}{(2\pi)^3 2E_5} \frac{d^3 p_6}{(2\pi)^3 2E_6} \\ &\times (2\pi)^4 \delta^4 \left( \sum_i p_i - \sum_f p_f \right), \end{aligned} \quad (6)$$

where  $p_i = p_1, p_2$  are the momenta of incoming fermions and  $p_f = p_3, p_4, p_5, p_6$  are the momenta of outgoing fermions.  $|M|^2$  is the square of the full amplitude which is averaged over initial spins and summed over final spins. By rearranging the top quark propagator, the full amplitude can be expressed as follows:

$$|M|^2 (2\pi)^4 \delta^4 \left( \sum_i p_i - \sum_f p_f \right) = \int \frac{d^4 q}{(2\pi)^4} \left| \sum_{s_t} M_a(s_t) D_t(q^2) M_b(s_t) \right|^2 (2\pi)^4 \delta^4(p_1 + p_2 - q - p_3) (2\pi)^4 \delta^4(q - p_4 - p_5 - p_6), \quad (7)$$

where  $q$  and  $s_t$  are the internal momentum and spin of the top quark.  $D_t(q^2)$  is the Breit-Wigner propagator factor for the  $t$  quark

$$D_t(q^2) = \frac{1}{q^2 - m_t^2 + im_t \Gamma_t}. \quad (8)$$

Here  $M_a(s_t)$  is the amplitude for  $e^+ b \rightarrow t \bar{\nu}$  with on shell  $t$  quark.  $M_b(s_t)$  is the decay amplitude of the  $t$  quark which will be given later. Using the narrow width approximation differential cross section becomes

$$d\sigma(e^+ b \rightarrow t \bar{\nu} \rightarrow \ell^+ b \bar{\nu} \nu_\ell) = \frac{1}{2s} \frac{1}{(2m_t \Gamma_t)} \left| \sum_{s_t} M_a(s_t) M_b(s_t) \right|^2 \frac{d^3 p_3}{(2\pi)^3 2E_3} \frac{d^3 q}{(2\pi)^3 2E_t} (2\pi)^4 \delta^4(p_1 + p_2 - p_3 - q) \\ \times \frac{d^3 p_4}{(2\pi)^3 2E_4} \frac{d^3 p_5}{(2\pi)^3 2E_5} \frac{d^3 p_6}{(2\pi)^3 2E_6} (2\pi)^4 \delta^4(q - p_4 - p_5 - p_6), \quad (9)$$

where  $M_a(s_t)$  indicates average over initial fermion spins, summation over final state fermion spins except  $t$  quark.  $M_b(s_t)$  indicates summation over final state fermion spins only. Therefore the full cross section has been written as a product of production and decay parts. One can show that interference terms from different spin states will vanish after integrating the decay part over azimuthal angles of top quark decay products. Then, the following result can be reached:

$$d\sigma(e^+ b \rightarrow t \bar{\nu} \rightarrow \ell^+ b \bar{\nu} \nu_\ell) = \left[ d\sigma(e^+ b \rightarrow \uparrow t \bar{\nu}) \frac{d\Gamma(\uparrow t \rightarrow \ell b \nu_\ell)}{\Gamma(t \rightarrow \ell b \nu_\ell)} + d\sigma(e^+ b \rightarrow \downarrow t \bar{\nu}) \frac{d\Gamma(\downarrow t \rightarrow \ell b \nu_\ell)}{\Gamma(t \rightarrow \ell b \nu_\ell)} \right] \text{BR}(t \rightarrow \ell b \nu_\ell), \quad (10)$$

where  $\text{BR}(t \rightarrow \ell b \nu_\ell)$  is the leptonic branching ratio for the top quark. For partial top polarization  $d\Gamma(t \rightarrow \ell b \nu_\ell) = d\Gamma(\uparrow t \rightarrow \ell b \nu_\ell) + d\Gamma(\downarrow t \rightarrow \ell b \nu_\ell)$  and up or down arrows indicate spin up or spin down cases along a specified spin quantization axis.

The square of the decay amplitude for  $t \rightarrow \ell b \nu_\ell$  for the polarized top quark including anomalous couplings is given below:

$$|M_b|^2 = -(p_b \cdot p_\ell - p_b \cdot p_t)(p_\ell \cdot p_t - m_t(s_t \cdot p_\ell)) + F_{2R}[m_t^3(p_b \cdot p_\ell) - 2m_t(p_b \cdot p_\ell)^2 + 2m_t(p_b \cdot p_\ell)(p_b \cdot p_t) \\ + 2m_t(p_b \cdot p_\ell)(p_\ell \cdot p_t) - 4m_t(p_b \cdot p_t)(p_\ell \cdot p_t) + m_t^2(p_\ell \cdot p_t)(s_t \cdot p_b) - 2(p_b \cdot p_\ell)(p_\ell \cdot p_t)(s_t \cdot p_b) \\ + 2(p_b \cdot p_t)(p_\ell \cdot p_t)(s_t \cdot p_b) - 2(p_\ell \cdot p_t)^2(s_t \cdot p_b) - 4m_t^2(p_b \cdot p_\ell)(s_t \cdot p_\ell) + 3m_t^2(p_b \cdot p_t)(s_t \cdot p_\ell) \\ + 2(p_b \cdot p_\ell)(p_b \cdot p_t)(s_t \cdot p_\ell) - 2(p_b \cdot p_t)^2(s_t \cdot p_\ell) + 2(p_b \cdot p_t)(p_\ell \cdot p_t)(s_t \cdot p_\ell)] / (2M_W) - F_{2R}^2[2m_t^4(p_b \cdot p_\ell) \\ - 4m_t^2(p_b \cdot p_\ell)^2 + m_t^2(p_b \cdot p_\ell)(p_b \cdot p_t) + 2(p_b \cdot p_\ell)^2(p_b \cdot p_t) - 2(p_b \cdot p_\ell)(p_b \cdot p_t)^2 - 5m_t^2(p_b \cdot p_t)(p_\ell \cdot p_t) \\ + 4(p_b \cdot p_\ell)(p_b \cdot p_t)(p_\ell \cdot p_t) + 2(p_b \cdot p_t)^2(p_\ell \cdot p_t) + 2(p_b \cdot p_t)(p_\ell \cdot p_t)^2 - 3m_t^3(p_b \cdot p_\ell)(s_t \cdot p_b) \\ + 2m_t(p_b \cdot p_\ell)^2(s_t \cdot p_b) - 2m_t(p_b \cdot p_\ell)(p_b \cdot p_t)(s_t \cdot p_b) + m_t^3(p_\ell \cdot p_t)(s_t \cdot p_b) + 6m_t(p_b \cdot p_t)(p_\ell \cdot p_t)(s_t \cdot p_b) \\ - 2m_t(p_\ell \cdot p_t)^2(s_t \cdot p_b) - 4m_t^3(p_b \cdot p_\ell)(s_t \cdot p_\ell) + 2m_t^3(p_b \cdot p_t)(s_t \cdot p_\ell) + 4m_t(p_b \cdot p_\ell)(p_b \cdot p_t)(s_t \cdot p_\ell) \\ - 4m_t(p_b \cdot p_t)^2(s_t \cdot p_\ell) + 4m_t(p_b \cdot p_t)(p_\ell \cdot p_t)(s_t \cdot p_\ell)] / (4M_W^2) - F_{2L}^2[2m_t^4(p_b \cdot p_\ell) + 4m_t^2(p_b \cdot p_\ell)^2 \\ - 5m_t^2(p_b \cdot p_\ell)(p_b \cdot p_t) - 2(p_b \cdot p_\ell)^2(p_b \cdot p_t) + 2(p_b \cdot p_\ell)(p_b \cdot p_t)^2 + m_t^2(p_b \cdot p_t)(p_\ell \cdot p_t) \\ - 4(p_b \cdot p_\ell)(p_b \cdot p_t)(p_\ell \cdot p_t) - 2(p_b \cdot p_t)^2(p_\ell \cdot p_t) - 2(p_b \cdot p_t)(p_\ell \cdot p_t)^2 + m_t^3(p_b \cdot p_\ell)(s_t \cdot p_b) \\ + 2m_t(p_b \cdot p_\ell)^2(s_t \cdot p_b) - 2m_t(p_b \cdot p_\ell)(p_b \cdot p_t)(s_t \cdot p_b) + m_t^3(p_\ell \cdot p_t)(s_t \cdot p_b) - 2m_t(p_b \cdot p_t)(p_\ell \cdot p_t)(s_t \cdot p_b) \\ - 2m_t(p_\ell \cdot p_t)^2(s_t \cdot p_b) - 4m_t^3(p_b \cdot p_\ell)(s_t \cdot p_\ell) - 2m_t^3(p_b \cdot p_t)(s_t \cdot p_\ell) + 4m_t(p_b \cdot p_\ell)(p_b \cdot p_t)(s_t \cdot p_\ell) \\ + 4m_t(p_b \cdot p_t)^2(s_t \cdot p_\ell) + 4m_t(p_b \cdot p_t)(p_\ell \cdot p_t)(s_t \cdot p_\ell)] / (4M_W^2). \quad (11)$$

In the case of the standard model, the angular distributions of the top decay products have a simple correlation with the top quark spin

$$\frac{1}{\Gamma} \frac{d\Gamma(\lambda)}{d(\cos\theta)} = \frac{1}{2}(1 + \lambda\alpha_i \cos\theta), \quad (12)$$

where  $\alpha_i = 1$  for the outgoing charged lepton which has the strongest correlation. Here subscript  $i$  refers to decay products of the top quark and  $\theta$  is the angle between the charged lepton momentum and the top spin quantization axis in the rest frame of the top quark. The decay rate  $\Gamma$  stands for  $\Gamma(t \rightarrow \ell b \nu_\ell)$  and  $\lambda = \mp 1$  for up and down spin states. The curves in Fig. 1 show the angular distributions of the charged lepton including anomalous couplings. From Fig. 1 we see that the decay rate is far more sensitive to the coupling  $F_{2R}$  than to the  $F_{2L}$ . The reason for this is understood from the amplitude above that the decay rate depends on the  $F_{2R}$  with the first and the second power while it depends on the  $F_{2L}$  with the second power only. From the integration over  $\cos\theta$ , it is seen that the total decay rate  $\Gamma$  is independent of spin polarization for a fixed decomposition axis. So, after the phase space integration over the decay products of the top quark, the full cross section takes the form of the known unpolarized cross section,

$$\begin{aligned} d\sigma(e^+ b \rightarrow t \bar{\nu} \rightarrow \ell^+ b \bar{\nu} \nu_\ell) &= [d\sigma(e^+ b \rightarrow \uparrow t \bar{\nu}) \\ &+ d\sigma(e^+ b \rightarrow \downarrow t \bar{\nu})] \\ &\times BR(t \rightarrow \ell b \nu_\ell). \end{aligned} \quad (13)$$

Once the experimental measurement of the angular distributions of outgoing charged lepton has been performed in the top rest frame, one can determine the polarization of the top quark. Then it is possible to obtain from the expression (10) the polarized production cross section as a coefficient of the angular distribution by fitting procedure. However, this is unavailable due to an ambiguity in

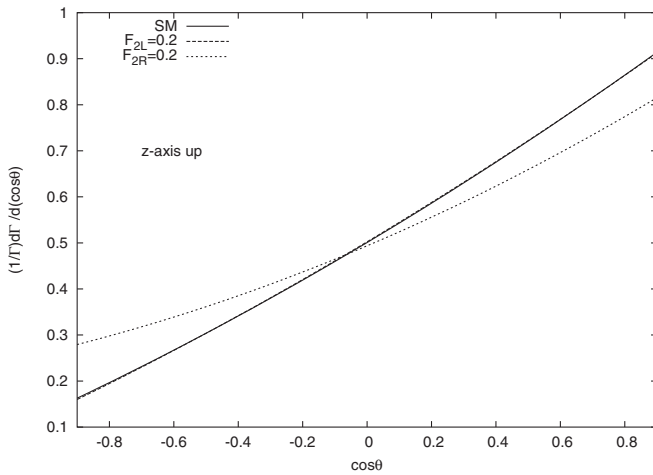


FIG. 1. Angular distributions of the charged lepton for polarized top decay with anomalous  $Wtb$  couplings shown in the figure. The top spin up is chosen along the  $z$  axis. The curve for  $F_{2R} = 0$ ,  $F_{2L} = 0.2$  is almost coincident with the SM one.

reconstructing the top four momentum. That is why we need to use the top production cross section for estimating sensitivity of  $ep$  collision to anomalous couplings.

The top spin dependent squared amplitude with initial spins averaged for the top quark production subprocess  $e^+ b \rightarrow t \bar{\nu}$  is written below:

$$A_1 = -\left[\hat{u} + \frac{\hat{s}\hat{t}F_{2R}^2}{M_W^2}\right][p_e \cdot p_t - m_t p_e \cdot s_t] \quad (14)$$

$$A_2 = -\frac{\hat{u}\hat{t}F_{2L}^2}{2M_W^2}[m_t^2 - 2m_t p_{\bar{\nu}} \cdot s_t - \hat{s}] \quad (15)$$

$$A_3 = -\frac{\hat{u}F_{2L}}{M_W}[-m_t^2 p_e \cdot s_t + m_t \hat{t} - \hat{s} p_b \cdot s_t - \hat{t} p_{\bar{\nu}} \cdot s_t] \quad (16)$$

$$|M_a|^2 = \frac{1}{4} \frac{g_w^4}{(k^2 - M_W^2)^2} (A_1 + A_2 + A_3), \quad (17)$$

where momentum of the each particle is represented by its symbol and  $\hat{s}$ ,  $\hat{t}$ , and  $\hat{u}$  are Mandelstam invariants for the subprocess. The momentum transfer  $k$  and top quark spin vector are defined by

$$\begin{aligned} k &= p_b - p_t & s_t^\mu &= \left( \frac{\vec{p}_t \cdot \vec{s}'}{m_t}, \vec{s}' + \frac{\vec{p}_t \cdot \vec{s}'}{m_t(E_t + m_t)} \vec{p}_t \right) \\ (s_t^\mu)_{\text{RS}} &= (0, \vec{s}'), \end{aligned} \quad (18)$$

where RS stands for the rest system of the top quark. The definition of the spin axis in the rest frame of the top quark does not depend on the coordinate system where the cross section is performed. So it is more convenient to calculate cross section in the center of mass system of incoming positron and  $b$  quark. In the top rest frame, its spin direction along the positron beam can be defined as follows:

$$\vec{s}' = \lambda \frac{\vec{p}_e^*}{|\vec{p}_e^*|}, \quad \lambda = \pm 1, \quad (19)$$

where  $\vec{p}_e^*$  is the positron momentum observed in the rest frame of the top quark. Since positron momentum  $\vec{p}_e$  is first defined in the cm system where the cross section is calculated, one should apply Lorentz boost to the rest frame of the top quark with the expression below:

$$\vec{p}_e^* = \vec{p}_e + \frac{\gamma - 1}{\beta^2} (\vec{\beta} \cdot \vec{p}_e) \vec{\beta} - E_e \gamma \vec{\beta}, \quad (20)$$

in which  $\vec{\beta}$  is the velocity of the top quark in the cm system and  $\beta^2$  can be written in terms of  $\hat{s}$  and  $m_t$ :

$$\vec{\beta} = \frac{\vec{p}_t}{E_t}, \quad \beta^2 = \frac{(\hat{s} - m_t^2)^2}{(\hat{s} + m_t^2)^2}, \quad \gamma = \frac{1}{\sqrt{1 - \beta^2}}. \quad (21)$$

In the case of the standard model, only the  $A_1$  term above contributes to the cross section. From  $|M_a|^2$  it is easy to show that the top quark is completely polarized in the direction of the  $e$ -beam. When anomalous couplings are included, it is seen that  $F_{2R}$  appears only in the term  $A_1$ . If down polarization in the  $e$ -beam basis is considered the term  $A_1$  is ineffective. The remaining terms  $A_2$  and  $A_3$  have the coupling only  $F_{2L}$ . The prominent difference between the production cross section for  $e^+b \rightarrow t\bar{\nu}$  and the decay rate is that the cross section  $\sigma(e^+b \rightarrow t\bar{\nu})$  includes the first and the second power of  $F_{2L}$  but only the second power of  $F_{2R}$ . The decay rate contains just the inverse. For coupling values  $F_{2R}, F_{2L}$  less than one, terms with first powers of couplings are more sensitive.

In order to see the influence of the anomalous couplings  $F_{2L}, F_{2R}$  on the integrated total cross section  $\sigma(e^+p \rightarrow t\bar{\nu} \rightarrow \ell^+b\bar{\nu}\nu_\ell)$ , we plot  $\sigma(e^+p \rightarrow \uparrow t\bar{\nu})$  and  $\sigma(e^+p \rightarrow \downarrow t\bar{\nu})$  in Figs. 2 and 3 as functions of anomalous couplings at TESLA + HERAp energy  $\sqrt{s} = 1.6$  TeV for a spin basis

along the proton beam. Here, polarized cross sections are calculated in the Lab frame which is the center of mass frame of the  $ep$  system. Figure 2 shows that the polarized cross sections have remarkably different behavior as a function of anomalous coupling  $F_{2L}$  when compared to the unpolarized one.

Polarization dependent angular distributions of top quarks  $\frac{d\sigma(e^+p \rightarrow \uparrow t\bar{\nu})}{d\cos\theta}$  and  $\frac{d\sigma(e^+p \rightarrow \downarrow t\bar{\nu})}{d\cos\theta}$  are presented in Figs. 4–6 for anomalous  $Wtb$  couplings  $F_{2L} = 0.2$  and  $F_{2R} = 0.2$  to see the comparison with unpolarized ones. Angular distributions are given in the center of mass frame of the  $eb$  system. For illustration only the incoming proton basis is considered in these figures. Down polarized top distributions in Fig. 5 look similar in shape and magnitude to the unpolarized ones in Fig. 6. But the behavior of the up polarized top distributions has a little difference in shape with lower magnitude of the cross section. Parton distribution functions of Martin, Roberts, and Stirling (MRST2002) [20] have been used.

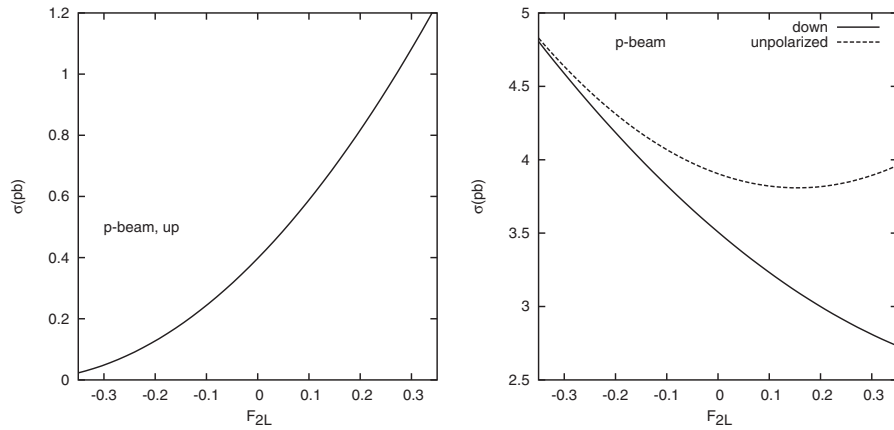


FIG. 2. Behavior of the unpolarized and polarized integrated total cross sections as a function of anomalous  $Wtb$  coupling  $F_{2L}$ . Top quark spin decomposition axis is along the  $p$ -beam.

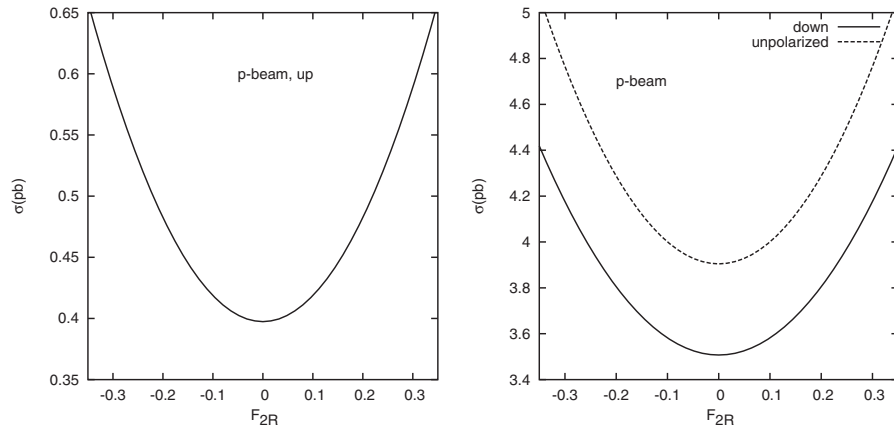


FIG. 3. The same as in the previous figure but for the anomalous  $Wtb$  coupling  $F_{2R}$ .

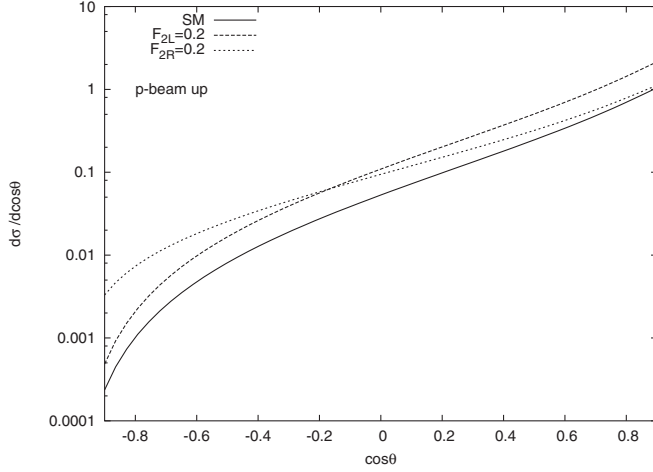


FIG. 4. Angular distribution of spin up polarized top quark for the anomalous  $Wtb$  coupling  $F_{2L} = 0.2$  or  $F_{2R} = 0.2$  when the top quark spin decomposition axis is along the proton beam. Each time only one of the  $Wtb$  couplings is different from the SM value.

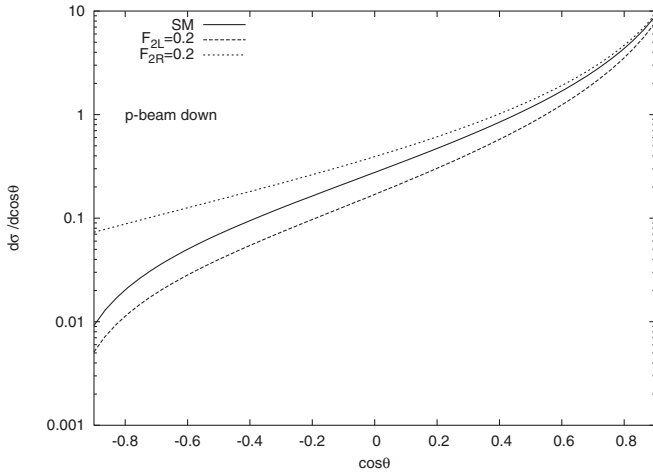


FIG. 5. The same as in the previous figure but for the top quark polarized along the opposite direction of the  $p$ -beam.

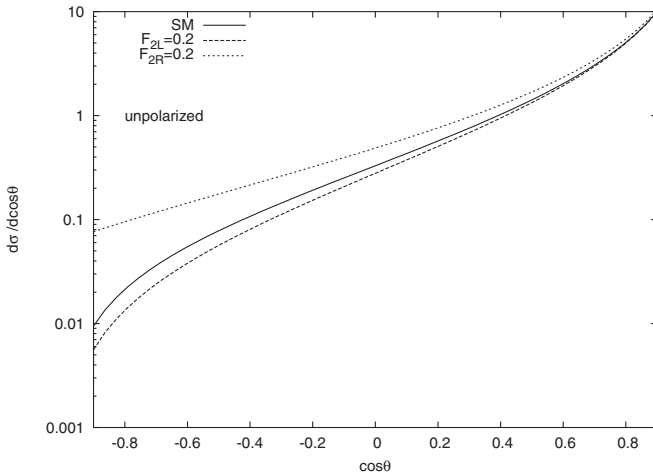


FIG. 6. The same as in the previous figure but for the unpolarized top quark.

### III. SENSITIVITY TO ANOMALOUS COUPLINGS

We use the simple  $\chi^2$  criterion from angular distributions of the top quark to estimate sensitivity of  $ep$  collision to anomalous  $Wtb$  couplings,

$$\chi^2 = \sum_{i=\text{bins}} \left( \frac{X_i - Y_i}{\Delta_i^{\text{exp}}} \right)^2, \quad (22)$$

$$X_i = \int_{z_i}^{z_{i+1}} \frac{d\sigma^{\text{SM}}}{dz} dz, \quad Y_i = \int_{z_i}^{z_{i+1}} \frac{d\sigma^{\text{NEW}}}{dz} dz, \quad (23)$$

$$\Delta_i^{\text{exp}} = X_i \sqrt{\delta_{\text{stat}}^2 + \delta_{\text{sys}}^2}, \quad z = \cos\theta. \quad (24)$$

We have divided the range of  $\cos\theta$  into 6 pieces and have considered at least 20 events in each bin. The expected number of events in the  $i$ th bin has been calculated considering the leptonic channel of  $W$  boson as the signal  $N_i = \epsilon L_{\text{int}} \sigma_i \text{BR}(W \rightarrow \ell + \nu)$ , where  $\epsilon$  is the overall efficiency and  $L_{\text{int}}$  is the integrated luminosity. The limits on the anomalous couplings  $F_{2L}$  and  $F_{2R}$  are provided in Table II at TESLA + HERAp energy  $\sqrt{s} = 1.6$  TeV for the deviation from the SM values at 95% confidence level with and without systematic error. The integrated luminosity and overall efficiency are taken into account as  $L_{\text{int}} = 20000 \text{ pb}^{-1}$  and  $\epsilon = 0.5$ . Only one of the couplings is assumed to deviate from the SM at a time. The only exception for the calculation of sensitivity is the down polarization of the top quark in the  $e$ -beam basis. There

TABLE II. Sensitivity of TESLA + HERAp collider to anomalous  $Wtb$  couplings at 95% C.L. for the decomposition axis of the top quark spin is along the  $e$ -beam,  $p$ -beam, and helicity directions. Only one of the couplings is assumed to deviate from the SM at a time. (P) indicates Poisson data in the absence of background.

Spin	$\delta^{\text{sys}}$	$F_{2L}$	$F_{2R}$
<i>e</i> -beam			
Up	0	-0.04, 0.04	-0.06, 0.06
Up	0.10	-0.07, 0.07	-0.07, 0.07
Down	0	0.03, 0.03 (P)	...
<i>p</i> -beam			
Up	0	-0.02, 0.01	-0.08, 0.08
Up	0.10	-0.03, 0.03	-0.09, 0.09
Down	0	-0.02, 0.02	-0.06, 0.06
Down	0.10	-0.04, 0.05	-0.07, 0.07
Helicity			
Up	0	-0.02, 0.02	-0.06, 0.06
Up	0.10	-0.04, 0.05	-0.07, 0.07
Down	0	-0.02, 0.02	-0.08, 0.08
Down	0.10	-0.04, 0.04	-0.09, 0.09
Unpol	0	-0.04, 0.04	-0.06, 0.06
Unpol	0.10	-0.06, 0.09	-0.07, 0.07

are two advantages of this case. First, the coupling  $F_{2R}$  does not contribute to the cross section and there remains just one type of coupling  $F_{2L}$  to be determined. Second, there is no standard model background and these are all events of the desired type. In order to obtain limits on the  $F_{2L}$ , we use the Poisson variable with 5 events to be observed. The next good improvement arises from the case where the polarization axis is along the  $p$ -beam. Without systematic error, the up polarization improves the limits on  $F_{2L}$  with a factor of 2.8 and down polarization with a factor of 2 when compared to the unpolarized one. These improvements reduce to 2.5 and 1.7 with systematic error 0.10. The up or down polarization does not improve

the limits on the  $F_{2R}$ . Similar features can be observed for the polarization in the helicity basis. It is straightforward to obtain similar results for antitop quarks with the process  $e^- p \rightarrow \bar{t} \nu$ .

Improved results by polarization in  $ep$  colliders have higher potential to probe  $F_{2L}$  and  $F_{2R}$  with high cross section and controllable background than Tevatron and LHC [9]. In order to compare  $ep$  colliders with the  $\gamma e$  mode of linear  $e^+e^-$  collider [7], hadronic channels should be included with more reduced uncertainties.

For more precise results, further analysis needs to be supplemented by observables with a more detailed knowledge of the experimental performances.

- 
- [1] H. Abramowicz *et al.*, DESY Report No. DESY-01-011FB, 2001 (unpublished).
- [2] S. Ambrosanio and B. Mele, *Z. Phys. C* **63**, 63 (1994).
- [3] N. V. Dokholian and G. V. Jikia, *Phys. Lett. B* **336**, 251 (1994).
- [4] K. Hagiwara, M. Tanaka, and T. Stelzer, *Phys. Lett. B* **325**, 521 (1994); E. Boos *et al.*, *Phys. Lett. B* **326**, 190 (1994).
- [5] E. Boos *et al.*, *Z. Phys. C* **70**, 255 (1996).
- [6] A. Bienarchik, K. Ciekiewicz, and K. Kolodziej, hep-ph/012253.
- [7] E. Boos, A. Pukhov, M. Sachwitz, and H. J. Schreiber, *Phys. Lett. B* **404**, 119 (1997).
- [8] D. Dicus and S. Willenbrock, *Phys. Rev. D* **34**, 155 (1986); C.-P. Yuan, *Phys. Rev. D* **41**, 42 (1990); G. V. Jikia and S. R. Slabospitsky, *Phys. Lett. B* **295**, 136 (1992); R. K. Ellis and S. Parke, *Phys. Rev. D* **46**, 3785 (1992); G. Bordes and B. van Eijk, *Z. Phys. C* **57**, 81 (1993); D. O. Carlson and C.-P. Yuan, *Phys. Lett. B* **306**, 386 (1993); G. Bordes and B. van Eijk, *Nucl. Phys.* **B435**, 23 (1995); S. Cortese and R. Petronzio, *Phys. Lett. B* **253**, 494 (1991); D. O. Carlson, E. Malkawi, and C.-P. Yuan, *Phys. Lett. B* **337**, 145 (1994); T. Stelzer and S. Willenbrock, *Phys. Lett. B* **357**, 125 (1995); R. Pittau, *Phys. Lett. B* **386**, 397 (1996); M. C. Smith and S. Willenbrock, *Phys. Rev. D* **54**, 6696 (1996); D. Atwood, S. Bar-Shalom, G. Eilam, and A. Soni, *Phys. Rev. D* **54**, 5412 (1996); C. S. Li, R. J. Oakes, and J. M. Yang, *Phys. Rev. D* **55**, 5780 (1997); G. Mahlon and S. Parke, *Phys. Rev. D* **55**, 7249 (1997); A. P. Heinson, A. S. Belyaev, and E. E. Boos, *Phys. Rev. D* **56**, 3114 (1997); T. Stelzer, Z. Sullivan, and S. Willenbrock, *Phys. Rev. D* **56**, 5919 (1997); D. Atwood, S. Bar-Shalom, G. Eilam, and A. Soni, *Phys. Rev. D* **57**, 2957 (1998); T. Stelzer, Z. Sullivan, and S. Willenbrock, *Phys. Rev. D* **58**, 094021 (1998); A. S. Belyaev, E. E. Boos, and L. V. Dudko, *Phys. Rev. D* **59**, 075001 (1999).
- [9] E. Boos, L. Dudko, and T. Ohl, *Eur. Phys. J. C* **11**, 473 (1999).
- [10] S. Atag, O. Cakir, and B. Dilec, *Phys. Lett. B* **522**, 76 (2001).
- [11] W. Buchmuller and D. Wyler, *Nucl. Phys.* **B268**, 621 (1986); K. Hagiwara, S. Ishihara, R. Szalapski, and D. Zeppenfeld, *Phys. Rev. D* **48**, 2182 (1993).
- [12] G. J. Gounaris, F. M. Renard, and C. Verzegnassi, *Phys. Rev. D* **52**, 451 (1995); G. J. Gounaris, F. M. Renard, and N. D. Vlachos, *Nucl. Phys.* **B459**, 51 (1996).
- [13] K. Whisnant, J. Yang, B. Young, and X. Zhang, *Phys. Rev. D* **56**, 467 (1997); J. M. Yang and B. Young, *Phys. Rev. D* **56**, 5907 (1997).
- [14] G. Kane, G. Ladinsky, and C.-P. Yuan, *Phys. Rev. D* **45**, 124 (1992).
- [15] M. S. Alam *et al.* (CLEO Collaboration), *Phys. Rev. Lett.* **74**, 2885 (1995); F. Larios, M. A. Perez, and C.-P. Yuan, *Phys. Lett. B* **457**, 334 (1999).
- [16] D. E. Groom *et al.*, *Eur. Phys. J. C* **15**, 1 (2000).
- [17] R. D. Peccei and X. Zhang, *Nucl. Phys.* **B337**, 269 (1990); R. D. Peccei, S. Peris, and X. Zhang, *Nucl. Phys.* **B349**, 305 (1991).
- [18] F. Olness and W.-K. Tung, *Nucl. Phys.* **B308**, 813 (1988); R. Barret, H. Haber, and D. Soper, *Nucl. Phys.* **B306**, 697 (1988); M. A. G. Aivazis, J. C. Collins, F. I. Olness, and W.-K. Tung, *Phys. Rev. D* **50**, 3102 (1994).
- [19] S. Atag and B. D. Sahin, *Phys. Rev. D* **70**, 037503 (2004).
- [20] A. D. Martin, W. J. Stirling, and R. G. Roberts, *Phys. Rev. D* **51**, 4756 (1995).